Identification of salicylic acid-independent responses in an Arabidopsis 3 phosphatidylinositol 4-kinase beta double mutant

Tetiana Kalachova, Martin Janda, Vladimír Šašek, Jitka Ortmannová, Pavla Nováková, Petre I Dobrev, Volodymyr Kravets, Anne Guivarc'H, Deborah Moura, Lenka Burketová, et al.

Original Article

Identification of salicylic acid-independent responses in an Arabidopsis phosphatidylinositol 4-kinase beta double mutant

KALACHOVA+ Tetiana[1,5], JANDA+ Martin[1,2], ŠAŠEK Vladimír[1], ORTMANNOVÁ Jitka[1,6], NOVÁKOVÁ Pavla[1,2], DOBREV I. Petre[1], KRAVETS Volodymyr[3], GUIVARC'H Anne[4], MOURA Deborah[5], BURKETOVÁ Lenka[1], VALENTOVÁ Olga[2], RUELLAND Eric[4,5*]

[1]Institute of Experimental Botany, The Czech Academy of Sciences, Prague 160 000, CZECH REPUBLIC

[2]University of Chemistry and Technology, Department of Biochemistry and Microbiology, Prague 166 28, CZECH REPUBLIC

[3]Institute of Bioorganic Chemistry and Petrochemistry National Academy of Sciences of Ukraine, 02094 Kyiv, UKRAINE

[4]CNRS, Institut d'Ecologie et des Sciences de l'Environnement de Paris, UMR 7618, Créteil, FRANCE

[5]Université Paris-Est, UPEC, Institut d'Ecologie et des Sciences de l'Environnement de Paris, Créteil, FRANCE

[6] current address - Department of Plant Biology, Swedish University of Agricultural Sciences, SE-750 07 Uppsala, SWEDEN

Running title: Salicylic acid-independent responses in PI4K mutants

* Corresponding author: Eric RUELLAND e-mail address: eric.ruelland@upmc.fr

+ Equally contributed

Abstract

Background and Aims

We have recently shown that an *Arabidopsis thaliana* double mutant of type III phosphatidylinositol-4-kinases (PI4Ks), *pi4kβ1β2*, constitutively accumulated a high level of salicylic acid (SA). By crossing this *pi4kβ1β2* double mutant with mutants impaired in SA synthesis (such as *sid2* impaired in isochorismate synthase) or transduction, we demonstrated that the high SA level was responsible for the dwarfism phenotype of the double mutant. Here we aimed at distinguishing between the SA-dependent and -independent effects triggered by the deficiency in *PI4Kβ1* and *PI4Kβ2*.

Methods

To achieve this, the *sid2pi4kβ1β2* triple mutant was a tool of choice. High-throughput analyses of phytohormones were performed on this mutant together with *pi4kβ1β2* and *sid2* mutants and wild-type plants. Responses to pathogens, namely *Hyaloperonospora arabidopsidis*, *Pseudomonas syringae* and *Botrytis cinerea*, but as well to the non-host fungus *Blumeria graminis*, were also determined. Callose accumulation was monitored in response to flagellin.

Key Results

We show here the prominent role of high SA levels in influencing the concentration of many other tested phytohormones, including abscisic acid and its derivatives, the Aspartate-conjugated form of indole-3-acetic acid and some cytokinins such as *cis*-zeatin. We show that the increased resistance of *pi4kβ1β2* plants to the host pathogens *Hyaloperonospora arabidopsidis*, *Pseudomonas syringae* pv. *tomato* DC3000 and *Bothrytis cinerea* is dependent on accumulation of high SA level. In contrast, accumulation of callose in *pi4kβ1β2* after

flagellin treatment was independent of SA. Concerning the response to *Blumeria graminis*, both callose accumulation and fungal penetration were enhanced in the *pi4kβ1β2* double mutant compared to wild-type plants. Both of these processes occurred in a SA-independent manner.

Conclusions

Our data extensively illustrate the influence of SA on other phytohormone levels. The *sid2pi4kβ1β2* triple mutant allowed to uncover the role of PI4Kβ1/β2 *per se*, thus showing the importance of these enzymes in plant defence responses.

Key words: pi4kβ1β2 / PI4Ks, callose, salicylic acid, phytohormones, isochorismate synthase 1, biotic stress, pathogens, *Arabidopsis thaliana*

INTRODUCTION

Salicylic acid (SA) is a phytohormone playing a role in many plant physiological processes although its role is mainly documented in plant response to biotic stress when SA accumulates within tissues, both at the site of attack and in a systemic manner (Vlot et al. 2009; Janda 2015). In plants, SA is biosynthesized via two pathways. One is dependent on phenylalanine ammonia-lyase (PAL; EC 4.3.1.24) which catalyses the conversion of phenylalanine to *trans*-cinnamic acid. In the other pathway, the key enzyme is ISOCHORISMATE SYNTHASE (ICS; EC 5.4.4.2) which catalyses the isomerization of chorismate into isochorismate (Dempsey et al. 2011). The ICS-dependent pathway was shown to be responsible for most SA accumulation upon pathogen attack. In *A. thaliana*, two ICS isoforms exist, but the major role in SA biosynthesis is played by ICS1. The *ICS1* mutant is known as *sid2* for *salicylic acid induction deficient 2* (Wildermuth et al. 2001; Wagner et al. 2013; Cui et al. 2017). When SA levels increase, downstream signalling events are triggered, and the best described molecular pathway is dependent on NONEXPRESSOR OF PATHOGENESIS RELATED 1 (NPR1). Upon SA action, homo-oligomeric NPR1 protein undergoes dissociation by reduction and the resulting monomers move into the nucleus where they interact with TGA-transcription factors to induce the expression of SA responsive genes. A NPR1 independent pathway also exists in response to SA (Janda 2015). The activation of SA signalling pathways leads to robust changes in the plant transcriptome, including defence related genes (Seyfferth and Tsuda 2014). Among the immune responses affected by changes in SA levels or by SA treatments is the accumulation of callose (Antignani et al. 2015; Dong et al. 2008; Kohler et al. 2002), a (1,3)-β-Glucan occurring in plant cell walls.

The signaling pathways triggered by SA are still the subject of current research. We have shown that phosphoinositides, the phosphorylated derivatives of phosphatidylinositol (PI), are involved in SA transduction. Indeed, PI can be phosphorylated at the D4 position of the

inositol ring by phosphatidylinositol-4-kinases (PI4K) thus leading to phosphatidylinositol 4-phosphate (PI4P); which can be phosphorylated further into phosphatidylinositol-4,5-bisphosphate (PI-4,5-P_2). There are two types of PI4Ks according to their primary sequences and pharmacological sensitivities. Type II PI4Ks are inhibited by adenosine while type III PI4Ks are inhibited by micromolar concentrations of wortmannin, a steroid metabolite produced by the fungus *Penicillium funiculosum* (Nakanishi et al. 1995, Balla 2007, Krinke et al. 2007). From the *A. thaliana* genome, twelve putative PI4K isoforms have been identified. Eight belong to type-II (AtPI4Kγ1-8), and four belong to type-III (AtPI4Kα1 and α2, AtPI4Kβ1 and β2) (Delage et al. 2012; Janda et al. 2013). We have shown that type III-PI4Ks are activated when *A. thaliana* suspension cells respond to SA, thus leading to an increase in PI4P and PI-4,5-P_2 (Krinke et al. 2007). PI-4,5-P_2 can act as a cofactor to some phospholipase Ds (Pappan et al. 1998). Interestingly, there is an overlap between SA responsive genes controlled by PI4Ks and those controlled by PLDs, leading to the working model that in response to SA, PI4P and PI-4,5-P_2 are produced with PI-4,5-P_2 acting as a cofactor for a PLD, whose product, PA, will trigger a signalling cascade (Krinke et al. 2009; Kalachova et al. 2016).

In order to better characterize the role of PI4Ks in the response to SA, we have used *A. thaliana* mutants altered in type III PI4Ks. We previously worked on a double mutant defective in the two PI4Kβ genes. Surprisingly, *pi4kβ1β2* exhibited a constitutively high SA level that resulted in constitutive high transcription of SA responsive genes such as *PR-1* (PATHOGENESIS RELATED 1). Therefore, PI4Ks are not only involved in SA transduction but they can also impact SA concentration. Furthermore, this double mutant exhibited dwarfism and was more resistant to the bacterial pathogen *Pseudomonas syringae* pv. *maculicola* ES4326 (Sasek et al. 2014). The *pi4kβ1β2* plant was crossed with mutants impaired in components of SA synthesis (*sid2*, impaired in *ICS1* expression; *eds1*), SA

transduction (*npr1*) or a mutant expressing bacterial SA-hydroxylase (NahG) that degrades SA to catechol. The resulting triple mutants allowed us to conclude that the dwarf phenotype of *pi4kβ1β2* plants was dependent on SA accumulation and its transduction *via* the NPR1 pathway (Janda et al. 2014; Sasek et al. 2014).

In the present study, our aim was to identify amongst the cellular and physiological processes affected by the deficiency of PI4Kβ1β2, those that were either SA-dependent or SA-independent. To achieve this, we used the *sid2pi4kβ1β2* triple mutant that does not accumulate SA and exhibits wild-type sized rosettes (Sasek et al. 2014). In this mutant, the effects of PI4Kß1 and PI4Kß2 mutations would not be masked by high SA levels. We showed that hormonal levels and pathogen resistance were mainly dependent on SA. However, we could show that *sid2pi4kβ1β2* plants accumulated higher amounts of callose in response to *flg22* and wounding. Interestingly, this SA–independent callose accumulation was also observed during early stages of interactions with *Blumeria graminis* when penetration was observed. Our data suggest that PI4Ks are involved in plant immune responses not only through SA accumulation but also via SA-independent processes.

MATERIALS AND METHODS

Plant material, growth conditions

In this study, we used the following genotypes of *A. thaliana*: Columbia-0 (WT), *sid2-3* (Gross et al. 2006), *npr1-1* (Cao et al. 1997) *NahG* (Delaney et al. 1994), *pi4kβ1β2* (SALK_040479 / SALK_09069; Preuss et al. 2006), *sid2pi4kβ1β2*, *NahGpi4kβ1β2*, and *npr1pi4kβ1β2* mutants previously described (Sasek et al. 2014).

All plants were cultivated in Jiffy 7 peat pellets at 22°C with 70% relative humidity. All plants were watered without additional fertilizers. As for the light regimes, plants were

routinely cultivated in daily cycles of 10 h light (100-130 µE m^{-2} s^{-1}) and 14 h dark. Plants that would be used for hormonal analysis or transcription analysis were cultivated under 16 h light (130-150 µE m^{-2} s^{-1}) and 8 h dark.

Pathogen i**noculation**

Two-week-old plants grown at high density in one pot were sprayed with *H. arabidopsidis* *NoCo2* spores (~100 spores/µl). The infected plants were cultivated in closed transparent plastic boxes in high humidity for 6 days under 16 h light/8 h dark (100-130 µE m^{-2} s^{-1}) at 19°C. For analysis, leaves collected from one pot were considered as one sample (for each genotype, 11 samples were analysed). Spores were counted under a microscope using a Bürker chamber and expressed as relative spore number in [%], where relative spore number for a given control genotype (WT or *sid2*) was set to 100%. The spores were counted as spores per mg of tissue fresh weight. The experiments [WT vs *pi4kβ1β2*] and [*sid2* vs *sid2pi4kβ1β2*] were conducted independently.

Inoculation with *Pseudomonas syringae* was performed according to (Katagiri et al. 2002) with modifications. Bacteria were cultivated overnight on King's B medium plates containing rifampicin (50 µg/µl). *Pseudomonas syringae* pv. *tomato* DC3000 (*Pst* DC3000) and *Pseudomonas syringae* pv. *tomato* DC3000 AvrRpt2 (*Pst* DC3000 AvrRpt2) were taken from the respective plate and resuspended in 10mM $MgCl_2$ to give an OD_{600}=0.001. Four-week-old plants were infiltrated with this suspension.

One disc (6 mm) from one leaf, three leaves at a similar developmental stage from one plant and three plants were collected as one sample of one genotype at 0 dpi and 3 dpi (3 dpi only for *Pst* DC3000; 2 dpi for *Pst* DC3000 AvrRpt2). Leaf discs were ground in 10mM $MgCl_2$ and decimal dilutions were performed. Colony forming units were counted.

Four-week-old *A. thaliana* plants were treated with 6 µl drops containing *Botrytis cinerea* BMM spores (5.10^4 spores/ml) by applying a single drop to each leaf, with three leaves at a

similar developmental stage inoculated for each plant. Treated plants were placed into closed plastic boxes and kept in low light (16h light/8h dark, 21°C; 10-20 µE m^{-2} s^{-1}) for 56 hpi.

Blumeria graminis f. sp. *hordei* (*Bgh*) was cultivated continuously on fresh barley (Golden promise) grown under short day conditions (19°C, 10/14 h, 50% humidity, at a light intensity of 70 µmol m^{-2} s^{-1}). Plants, approximately 4 weeks old, were inoculated by spreading spores from infected barley onto the adaxial side of their leaves (from leaf to leaf). The 5th - 6th leaves were cut off at selected hpi and cleared with 96% ethanol or chloral hydrate. For penetration rate, fungal structures were stained with 250 mg/ml trypan blue in a lactophenol/ethanol solution (Vogel and Somerville 2000). Stained leaves were observed by classical epifluorescence microscopy or bright-field microscopy using a Zeiss AxioImager ApoTome2 (objective 100x).

Callose deposition

Four-week-old *A. thaliana* plants were treated for 24 h with 100 nM flg22 or infiltrated with *Pst DC3000*. Distilled water infiltration was used as a control (mock) treatment. Infiltrated leaves were decolored in ethanol:glacial acetic acid (3:1 v/v). The leaves were then rehydrated in successive baths of 70% ethanol (at least 1 h), 50% ethanol (at least 1 h), 30% ethanol (at least 1 h) and water (at least 2h). Leaves were stained for 4 h with 0.01 % aniline blue in 150 mM K_2HPO_4, pH 9.5. Callose deposition was observed by fluorescence microscopy using a Zeiss AxioImager ApoTome2 (objective 10x). In the case of *Bgh* infection analysis, we calculated only callose spots using the high circularity function of the measurement settings at an interval of 0.5-1 which allowed us to distinguish only the cells with the size exclusion limit for spots corresponding to either encased haustoria or enormous papilla. Callose deposition was observed by fluorescence microscopy using a Zeiss AxioImager ApoTome2 (objective

10x). Images were processed with ImageJ software. At least four leaves from three independent plants were analysed for each variant.

RNA extraction and qPCR analysis

Plant tissues were homogenised in 2-ml screw-cap tubes containing 1 g of 1.3-mm diameter silica beads using a FastPrep-24 instrument (MP Biomedicals, Santa Ana, CA, USA). Total RNA was isolated using a Spectrum Plant Total RNA kit (Sigma-Aldrich, USA) and treated with a DNA-free kit (Ambion, USA). Subsequently, 1 μg of RNA was converted to cDNA with M-MLV RNase H–Point Mutant reverse transcriptase (Promega Corp., USA) and an anchored oligo dT21 primer (Metabion, Germany). Gene transcription was quantified by qPCR using a LightCycler 480 SYBR Green I Master kit and a LightCycler 480 (Roche, Switzerland). The PCR conditions employed were 95°C for 10 min followed by 45 cycles of 95°C for 10 s, 55°C for 20 s, and 72°C for 20 s. Melting curve analyses were then carried out. Relative transcription was normalized to the housekeeping genes *SAND* or *TIP41* (Czechowski et al. 2005). Primers were designed using PerlPrimer v1.1.21 (Marshall, 2004). The primers used were CalS1_FP, AAGAGCGGAGGGTCACTTTG; CalS1_RP, GGCGACACGAATAGACGGAT; CalS12_FP, TTCACTCCGTTTTCCCGAGG; CalS12_RP, GGAGAGAGACGCATCTGAGC.

Analysis of plant hormones

Plant hormones were extracted from 100 mg of frozen tissues and their concentrations were determined as previously described (Dobrev and Vankova 2012; Dobrev and Kaminek 2002) after the addition of appropriate internal standards. Hormone analysis was carried out on four samples, each taken from three plants. Briefly, samples were homogenized in tubes with 1.3 mm silica beads using a FastPrep-24 instrument (MP Biomedicals, USA). Samples were then

extracted with a methanol/H_2O/formic acid (15:4:1, v:v:v) mixture, which was supplemented with stable isotope-labeled phytohormone internal standards (10 pmol per sample) in order to check recovery during purification and to validate the quantification. The clarified supernatants were subjected to solid phase extraction using Oasis MCX cartridges (Waters Co., USA). The eluates were evaporated to dryness and the generated solids were dissolved in 30 µl of 15% (v/v) acetonitrile in water. Hormones were separated and quantified by Ultimate 3000 high-performance liquid chromatography (Dionex, Bannockburn, IL, USA) coupled to a 3200 Q TRAP hybrid triple quadrupole/linear ion trap mass spectrometer (Applied Biosystems, Foster City, CA, USA) as described by (Dobrev et al. 2017). Metabolite levels were expressed in pmol/g fresh weight (FW).

Statistical analysis

At least three independent biological replicates were performed for all experiments. Statistical analysis was conducted by paired *t*-test or ANOVA with Tukey honestly significant difference (HSD) multiple mean comparison *post hoc* test. The number of analysed samples was specified for each condition. The correlation matrix for hormonal levels was prepared using R-software *Hmisc* and *corrplot* packages based on the Pearson correlation (Team 2014).

RESULTS

The pi4kβ1β2 double mutant has altered phytohormonal levels

Our goal was to identify SA-dependent and SA-independent processes triggered by the double *pi4kβ1β2* mutation. To do so, we used a *sid2pi4kβ1β2* triple mutant. If a process triggered by the double *pi4kβ1β2* mutation is SA-dependent, then it should disappear in the *sid2pi4kβ1β2*

triple mutant. On the other hand, if a process triggered by the double *pi4kβ1β2* mutation is SA-independent, then it should still be observed in the *sid2pi4kβ1β2* triple mutant.

Since the main effect of the double *pi4kβ1β2* mutation was on the level of SA, we decided to quantify a broad spectrum of phytohormones in the *sid2pi4kβ1β2* triple mutant. The hormone levels obtained were compared to those of *pi4kβ1β2*, *sid2* and WT plants. A first look allowed us to establish that the *pi4kβ1β2* double mutation does not impact only SA levels. Many hormone-related metabolites showed significantly different levels in *pi4kβ1β2* plants when compared to WT plants while most of them remained at WT levels in *sid2pi4kβ1β2* (supplemental Table S1). In our previous study, we created an additional triple mutant by crossing *pi4kβ1β2* with a *NahG* mutant impaired in SA accumulation: *NahGpi4kβ1β2* (Sasek et al. 2014). To confirm and to strengthen the results obtained with *sid2pi4kβ1β2*, we also quantified phytohormones in *NahGpi4kβ1β2*, together with their corresponding single mutants (Supplemental table S1). From these data, we built a correlation matrix (Fig. 1). Many hormone levels were correlated to higher SA levels (Pearson correlation higher than 0.7) as seen for the abscisic acid (ABA) derivatives such as 9-hydroxy-ABA (9OH-ABA), phaseic acid (PA) and dihydrophaseic acid (DPA). However, the high levels of DPA, PA and 9OH-ABA observed in *pi4kβ1β2* versus WT were no longer seen in the triple mutants with low SA; therefore, these metabolite levels were controlled by SA in the *pi4kβ1β2* double mutant (Fig. S1A).

Since the main genetic pathway of SA response is controlled by NPR1, we investigated whether the hormonal control of SA was NPR1-dependent. This was achieved using a previously generated *npr1pi4kβ1β2* triple mutant where the SA level was 30-fold that of WT and 4-fold that of *pi4kβ1β2*. Interestingly, levels of DPA, PA and 9-OH were still high in *npr1pi4kβ1β2*, showing that the SA effect on these metabolites was only partially NPR1-dependent. It should be noted that ABA levels did not correlate with SA (Pearson correlation

0.3), thus indicating that the action of SA on ABA-derivatives is probably not directly connected with the biosynthesis of ABA, but with its metabolism.

Other hormones with high Pearson correlations to SA were the Asp conjugated form of indole-3-acetic acid (Asp-IAA) and some cytokinins. The increased level of IAA-Asp observed in *pi4kβ1β2* was no longer observed in the triple mutants with low SA. However, it was still visible in the *npr1pi4kβ1β2* triple mutant thus suggesting that this metabolite is controlled by SA but it is only partially NPR1-independent (Fig. S1B). The pattern of IAA was different from that of Asp-IAA, suggesting that SA control of Asp-IAA is on aspartate conjugation. As for cytokinins, the increase in *cis*-zeatin (cZ), *cis*-zeatin-riboside (cZR), *cis*-zeatin-7-N-glucoside (cZ7G), *cis*-zeatin-riboside-*O*-glucoside (cZROG) and *trans*-zeatin-*O*-glucoside (tZOG) and the decrease of *trans*-zeatin-7-N-glucoside (tZ7G) and *trans*-zeatin -9-N-glucoside (tZ9G) in the *pi4kβ1β2* double mutant was SA-driven. In contrast to the other hormones tested, SA action on tZROG appeared to be partially independent of NPR1 (Fig. S1C).

We identified one hormone for which its level was altered in *pi4kβ1β2* plants independently of SA. Indeed, the increase of oxIAA-GE observed in *pi4kβ1β2* was still visible in the triple mutants with low SA. It should be noted that oxIAA did not follow the same pattern (Fig. S2).

Pathogen resistance, including a necrotroph, of *pi4kβ1β2* plants is SA-dependent

At the hormonal level our data show that the major change induced by the *pi4kβ1β2* double mutation was an increase in SA, with this change determining the levels of many other

hormones. Since a major role of SA is related to biotic stress responses, we reasoned that processes related to biotic stress, dependent or not on SA, might also be altered in the double mutant.

Whether the PI4K double mutation *per se* was accompanied by an enhanced resistance to pathogens was investigated. Comparing resistance in *sid2pi4kβ1β2* plants to that in *pi4kβ1β2* or *sid2* would allow us to distinguish between the effectiveness of SA-dependent and independent responses. Therefore, different pathogens with different lifestyles (biotrophs, hemibiotrophs and necrotrophs) were tested (Glazebrook 2005). The *pi4kβ1β2* double mutant plants were more resistant to the biotroph *H. arabidopsidis NoCo2* compared to WT. However, *sid2pi4kβ1β2* resistance was similar to that of *sid2* plants (Fig. 2A). We then studied resistance to the hemibiotroph *Pseudomonas syringae* pv. *tomato* DC3000 in its wild type (*Pst* DC3000) or AvrRpt2 expressing form (*Pst* DC3000 AvrRpt2). *Pst* DC3000 AvrRpt2 leads to a strong effector triggered immunity (ETI) response compared to *Pst* DC3000. With both forms, pathogen development was reduced in *pi4kβ1β2* plants compared to the WT while *sid2pi4kβ1β2* resistance was comparable to that of *sid2* and lower than WT plants (Fig. 2B, Fig. S3). Unexpectedly, the double mutant also showed an increased resistance to the necrotroph *B. cinerea* which was also SA-dependent since *sid2pi4kβ1β2* resistance was similar to that of *sid2* and WT plants (Fig. 2C). For each pathogenic assay, triple mutant resistance was similar to *sid2*, indicating that SA-dependent pathways were dominant in the immune response. Putative mechanisms regulated by PI4K activity alone were not sufficient to establish pathogen resistance.

The enhanced level of basal callose deposition in *pi4kβ1β2* is mainly SA-dependent while stress-induced callose accumulation is not

SA levels modulate numerous processes associated with immune responses including the strengthening of leaf tissues and particularly cell walls around the infection site by lignification and callose accumulation (Voigt 2014). Interestingly, SA pre-treatment also has a positive effect on flagellin-induced callose accumulation (Yi et al. 2014). We therefore studied callose levels, accumulated in leaf tissues in response to treatment with the flagellin epitope (flg22). At first, we studied callose accumulation in the absence of flg22 treatment (control; Fig. 3A). The *pi4kβ1β2* double mutant exhibited a constitutively high level of callose deposition, as previously shown (Antignani et al. 2015). We were able to show that a spatial pattern in callose accumulation existed, since the examination of different regions of interest (ROI) indicated a higher accumulation in the upper part of the leaf edges (Fig. 3B).

Callose accumulation was then assessed in either mock-infiltrated or flg22-treated plants (Fig.4). In this case, callose accumulation was much higher in *pi4kβ1β2* when compared to WT plants (Fig. 4A, B). The *sid2pi4kβ1β2* triple mutant was used to investigate whether high callose deposition in the double mutant depended on its high SA level. For mock treatments, callose deposition was much lower in *sid2pi4kβ1β2* compared to *pi4kβ1β2* plants. This provides arguments for a SA-dependent higher basal callose deposition. This was confirmed by the response to flg22. In WT plants, flg22 induced 20-times more callose compared to control mock infiltrations. Again, the callose level in *pi4kβ1β2* was higher (2-fold) compared to WT plants. This increase was reduced when the *sid2* mutation was introduced into the *pi4kβ1β2* double mutant as the level in the triple mutant was *circa* 2-fold lower than in the double mutant and in the same range as the WT level. This indicated that SA was a major inducer of callose accumulation in the *pi4kβ1β2* genotype context. Yet, the *sid2pi4kβ1β2* triple mutant exhibited a higher callose deposition than *sid2* plants. Therefore, the *pi4kβ1β2* double mutation *per se* had a role in the high callose accumulation observed in the *pi4kβ1β2* double mutant.

We also studied callose accumulation in leaf tissues in response to mechanical wounding (Fig. S4). Again, in response to wounding, the PI4K double mutation enhanced callose accumulation via a SA-dependent pathway.

Whether callose overaccumulation correlated with the transcription of callose synthases (*CalSs*) was then investigated. Among 12 callose synthases, *CalS1*, *CalS12* have been shown to be related to SA and/or biotic stresses (Dong et al. 2008). The transcript levels of *CalS1* and *CalS12* were tested by qPCR in WT, *pi4kβ1β2*, *sid2* and *sid2pi4kβ1β2* plants treated or not with flg22. No correlation was observed between *CalS1* and *CalS12* transcript levels and callose accumulation (Fig. S5).

_pi4kβ1β2_ has altered non-host resistance that is SA-independent

The establishment of non-host resistance is based on different mechanisms, involving vesicular secretion as well as callose accumulation (Collins at al. 2003, Assaad et al. 2004, Takemoto et al. 2006, Bohlenius et al. 2010, Lee et al., 2017). To study the role of PI4K in such responses, we tested penetration success and callose production in response to the non-host pathogen *Blumeria graminis f. sp. hordei* (*Bgh*). In *Bgh*/*A. thaliana* interactions, callose accumulates in defensive papillae and haustorial encasements or around dead cells (Assaad et al. 2004, Ellinger et al. 2013, Jacobs et al., 2003). The enhanced number of plant cells with developed haustoria or dead cells reflects the penetration success of fungal hyphae (Fig. 5A). In our experiments a higher penetration correlated with greater callose accumulation in the plant tissue. In particular the *pi4kβ1β2* double mutant showed an enhanced successful penetration of *Bgh* 24 h post inoculation (hpi), as seen by the enhanced number of haustoria and dead cells. A similar defect in penetration resistance was seen in *sid2/pi4kβ1β2*, thus revealing the SA-independent character of this phenomenon (Fig. 5B). Both, *pi4kβ1β2* and *sid2/pi4kβ1β2* accumulated more callose (Fig. 5C) and over larger areas compared to WT

plants (Fig. 5C, D). Thus, the lower penetration resistance accompanied by callose accumulation in *pi4kβ1β2* was independent of the SA pathway.

DISCUSSION

The aim of this study was to investigate SA-dependent and -independent processes caused by the *pi4kβ1β2* double mutation. As previously shown (Sasek et al. 2014), this mutant accumulates a constitutively high level of SA. In *pi4kβ1β2*, SA biosynthesis is dependent on ISOCHORISMATE SYNTHASE 1 (ICS1), demonstrated by an absence of SA accumulation in the *sid2pi4kβ1β2* triple mutant with impaired *ICS1* transcription (Sasek et al. 2014). This was confirmed with the hormone analysis described in the present study. The *sid2pi4kβ1β2* triple mutant lacking high SA was used as a tool to distinguish between SA-dependent and SA-independent effects caused by the double mutation in *pi4kβ1β2*.

We first measured phytohormonal levels in fully developed leaves of four-week-old *A. thaliana* WT, *pi4kβ1β2*, *sid2* and *sid2pi4kβ1β2* plants. According to our knowledge, this is the broadest phytohormonal study carried out with a SA over-accumulating mutant (in our case *pi4kβ1β2*) and its comparison with a plant having the same background but with an impaired SA pathway (*sid2pi4kβ1β2*). The level of 15 hormone derivatives (excluding SA) was altered in *pi4kβ1β2* compared to WT leaves. For 13 of these, this was SA-dependent. We could identify two metabolites, *cis*-zeatin-riboside-5'-monophosphate and glucosylesters of oxindole-3-acetic acid, for which the *pi4kβ1β2* double mutation effect was SA-independent. The same conclusions were also reached with another triple mutant, *NahGpi4kβ1β2*. Amongst the hormones controlled by SA were ABA derivatives such as DPA, PA and 9OH-ABA. As ABA levels did not correlate with SA, the action of SA on ABA-derivatives did not appear to act on ABA biosynthesis but on its metabolism. Such an effect of SA on ABA catabolism is poorly described. A slight induction of ABA 8'-hydroxylase expression was observed after a

385 24 h SA treatment of rice seedlings (Mega et al. 2015). In an *A. thaliana cpr22* mutant
386 (*constitutive expressor of PR genes 22*), the increase of SA and ABA levels due to a high-low
387 humidity shift was also followed by the SA-dependent expression of genes encoding ABA
388 metabolising enzymes (Mosher et al. 2010).
389 Other hormones displaying a high correlation to SA were IAA-Asp and some cytokinins (SA
390 positively controlled cZROG and tZOG and negatively controlled tZ7G and tZ9G). The
391 pattern of IAA was different from that of IAA-ASP, suggesting that SA control of IAA-Asp
392 was on aspartate conjugation. Aspartate conjugation is catalysed by GH3.2-GH3.6 (Normanly
393 2010), with our transcriptome data obtained with *in vitro* grown *pi4kβ1β2* seedlings (Sasek et
394 al. 2014) indicating that *GH3.3* (At2g23170) was overexpressed in the double mutant. It
395 would be interesting to investigate whether it was responsible for the IAA-Asp/SA correlation
396 in our double mutant.
397 Our results demonstrate the major role of hormonal cross-talk between SA and other
398 hormones but only a minor role of impairment of PI4Kβ1/β2 *per se*. Since a major role of SA
399 is related to responses to biotic stresses, we reasoned that other processes related to biotic
400 stress, whether SA-dependent or not, could also be altered in the double mutant. We tested the
401 resistance of WT, *pi4kβ1β2*, *sid2* and *sid2pi4kβ1β2* plants against representative biotrophic
402 (oomycete *H. arabidopsidis* NoCo2), hemibiotrophic (bacteria *Pst* DC3000) and necrotrophic
403 (fungus *B. cinerea*) pathogens. Results clearly showed that resistance to these pathogens was
404 dependent on a high SA content. Resistance to *H. arabidopsidis* NoCo2 and *Pst* DC3000 was
405 perhaps not surprising as resistance to such pathogens is generally associated with SA
406 signalling (Glazebrook 2005). On the other hand, the role of SA in regulating resistance to
407 necrotrophs is rather uncommon. Indeed, plant defence against necrotrophs is commonly
408 associated with jasmonic acid signalling (Glazebrook 2005; Ferrari et al. 2003). However,
409 Ferrari et al. (2003) showed that resistance to *B. cinerea* could be dependent on high SA

levels, in accordance with our observations. A similar finding was reported for defence response to the necrotroph *Sclerotinia sclerotiorum* (Novakova et al. 2014). Moreover, we tested *A. thaliana* ETI by using a bacterial strain highly expressing the AvrRpt2 effector (*Pst* DC3000 AvrRpt2). An ETI response can induce the expression of genes commonly associated with SA, such as *PR-1*, in a SA-independent manner in *A. thaliana* (Tsuda et al. 2013). Yet, we found that the higher resistance of *pi4kβ1β2* plants against *Pst* DC3000 AvrRpt2 was SA-dependent. In conclusion, the higher resistance of *pi4kβ1β2* mutant against all the host pathogens assayed was strongly SA-dependent.

Non-host resistance, efficient against non-adapted pathogens, does not rely fully on the SA pathway. Here we show that *pi4kβ1β2* exhibited a SA-independent defective resistance towards penetration of the non-host pathogen *Bgh*.

Callose is a linear polysaccharide (1,3-β-glucan) occurring in plant cells where it is important for many plant physiological processes such as cytokinesis (Chen and Kim 2009). Callose accumulation is triggered in response to pathogens and is used as a common test of PTI upon treatment with typical PAMPs such as flg22, the epitope of flagellin (Luna et al. 2011). In mock inoculated *pi4kβ1β2*, callose deposition was greater than in WT leaves, thus confirming findings of Antignani et al. (2015). Interestingly, this was also true for the *sid2pi4kβ1β2* triple mutant when compared to *sid2* plants, thus indicating a SA-independent phenomenon. Following inoculation with flg22, an increase in callose deposition was observed in all genotypes tested, but this was still higher in *pi4kβ1β2* compared to WT leaves, and callose deposition was higher in *sid2pi4kβ1β2* with respect to *sid2* plants. Therefore, it seems that the *pi4kβ1β2* double mutation *per se* enabled higher callose deposition under biotic stress conditions.

The biosynthesis of callose occurs outside of the cell (Ellinger and Voigt 2014). Accumulation can be regulated at different levels: transcriptional, translational, or during

435 enzyme transport to the plasma membrane and out of the cell via vesicular trafficking.
436 Phosphorylation and direct translocation of callose synthase is crucial in the regulation of
437 biosynthesis, whereas transcriptional control might have only a minor role (Ellinger and Voigt
438 2014). Our data on the transcription levels of *CALS1* and *CALS12* indicate that in *pi4kβ1β2* a
439 transcriptional effect is not involved in the observed over accumulation of callose. So how is
440 it possible to explain the action on callose of the *pi4kβ1β2* double mutation *per se*? A number
441 of reports indicate that PI4Ks can impact trafficking. In *A. thaliana*, PI4Kβ1 was shown to be
442 recruited by the GTP bound Rab4b GTPAse. Both RabA4b and PI4Kβ1 localize to budding
443 secretory vesicles in the trans-golgi network (TGN) and to secretory vesicles *en route* to the
444 cell surface. A *pi4kβ1β2* double mutant produces secretory vesicles of highly variable sizes
445 (Antignani et al. 2015; Preuss et al. 2006; Kang et al. 2011). The product of PI4Ks activity,
446 PI4P massively accumulates at the plasma membrane and at early endosomes / TGN and
447 Golgi (Platre and Jaillais 2016; Noack and Jaillais 2017). Therefore PI4Kβ1/β2 are important
448 in vesicle trafficking. Interestingly, inhibiting PI4K with phenylarsine oxide (PAO)
449 suppressed the salt-induced endocytosis of plasma membrane intrinsic protein 2;1 (Ueda et
450 al., 2016). Similarly, inhibiting PI4K led to the internalization of CELLULOSE
451 SYNTHASE3 from the plasma membrane (Fujimoto et al. 2015). Can the impact of PI4K
452 betas on trafficking explain the increased callose accumulation? Callose biosynthesis and
453 accumulation have been shown to be affected by vesicle trafficking (Ellinger and Voigt
454 2014). PI4Ks has been shown to play an important role in cytokinesis (Lin et al. 2019),
455 especially in the correct organization of the vesicles at the cell division plane and further
456 formation of a cell plate. During phragmoplast formation, PI4Kβ1 likely interacts with
457 MPK4, a member of the MAP65 protein family that regulates microtubule organization (Lin
458 et al., 2019). Callose is also essential for cytokinesis (Thiele et al. 2009). We can therefore
459 only speculate whether the effects of PI4Ks on callose, cytokinesis and trafficking are

interconnected. Interestingly, the role of SA in these processes has not been tested. Since PI4Kβ1/β2 can impact the secretory pathway, they could also impact the translocation of callose synthases. Furthermore, PMR4 (CALS12) binds to small RabA4c GTPase at TGN and PI4Kβ1 binds to RabA4b GTPase, the most similar small GTPase to RabA4c, at TGN (Böhlenius et al., 2010). It should also be noted that the impact of PI4K betas on trafficking could also explain our non-host resistance data. The *syp121* mutant altered in a SNARE protein involved in trafficking has been reported to accumulate SA and also display defective non-host resistance (Collins et al., 2003).

In conclusion (Fig. 6), the *pi4kβ1β2* double mutant constitutively accumulated a high SA level via ICS1/SID2 and this had a big impact on other hormone levels and it was associated with an increased resistance to several plant pathogens (*P. syringae*, *H. arabidopsidis*, *B. cinerea*). The *pi4kβ1β2* double mutation also affected pathogen-related processes in a high SA-independent manner as seen by differences in callose accumulation in response to *flg22*, to *Bgh* infection, to wounding, and the higher penetration success of *Bgh*. The identification of such processes directly affected by the mutation on PI4Ks will now allow us to better investigate the role of these enzymes, in relation to signalling or trafficking events.

Funding information

This work was supported by the Czech Science Foundation [grant number. 17-05151S]. Collaboration of Ukrainian and French teams was partially supported by a “Projet international de coopération scientifique” from the “Centre National de la Recherche Scientifique” (2015-2018). TK received the Visegrad scholarship (2016-2017) [grant number 51600349]; she also benefited from the Program of Postdoctoral Fellowships of the Czech Academy of Sciences [grant number TK 919220]. The work was also supported by a European Regional Development Fund-Project "Centre for Experimental Plant Biology" [grant number CZ.02.1.01/0.0/0.0/16_019/0000738].

ACKNOWLEDGEMENTS

We thank Lucie Lamparová and Romana Pospíchalová for their technical support and Michael Hodges for language editing.

LITERATURE CITED

Antignani V, Klocko AL, Bak G, Chandrasekaran SD, Dunivin T, Nielsen E. 2015. Recruitment of PLANT U-BOX13 and the PI4Kbeta1/beta2 phosphatidylinositol-4 kinases by the small GTPase RabA4B plays important roles during salicylic acid-mediated plant defense signaling in Arabidopsis. *Plant Cell*, **27,** 243-61.

Assaad, F. F., Qiu, J. L., Youngs, H., Ehrhardt, D., Zimmerli, L., Kalde, M., ... & Somerville, C. R. (2004). The PEN1 syntaxin defines a novel cellular compartment upon fungal attack and is required for the timely assembly of papillae. Molecular biology of the cell, 15(11), 5118-5129.

Balla T. 2007. Imaging and manipulating phosphoinositides in living cells. *Journal of Physiology*, **582**, 927–937.

Böhlenius, H., Mørch, S. M., Godfrey, D., Nielsen, M. E., & Thordal-Christensen, H. (2010). The multivesicular body-localized GTPase ARFA1b/1c is important for callose deposition and ROR2 syntaxin-dependent preinvasive basal defense in barley. The Plant Cell, tpc-110.

Cao H, Glazebrook J, Clarke JD, Volko S, Dong X. 1997. The Arabidopsis NPR1 gene that controls systemic acquired resistance encodes a novel protein containing ankyrin repeats. *Cell,* **88,** 57-63.

Collins NC, Thordal-Christensen H, Lipka V, *et al.* 2003. SNARE-protein-mediated disease resistance at the plant cell wall. *Nature,* **425,** 973-7.

Cui H, Gobbato E, Kracher B, Qiu J, Bautor J, Parker JE. 2017. A core function of EDS1 with PAD4 is to protect the salicylic acid defense sector in Arabidopsis immunity. *New Phytologist,* **213,** 1802-1817.

Czechowski T, Stitt M, Altmann T, Udvardi MK, Scheible WR. 2005. Genome-wide identification and testing of superior reference genes for transcript normalization in Arabidopsis. *Plant Physiology,* **139,** 5-17.

Delage E, Ruelland E, Guillas I, Zachowski A, Puyaubert J. 2012. Arabidopsis type-III phosphatidylinositol 4-kinases beta1 and beta2 are upstream of the phospholipase C pathway triggered by cold exposure. *Plant and Cell Physiology,* **53,** 565-76.

Delaney TP, Uknes S, Vernooij B, *et al.* 1994. A central role of salicylic Acid in plant disease resistance. *Science,* **266,** 1247-50.

Dobrev PI, Hoyerova K, Petrasek J. 2017. Analytical Determination of Auxins and Cytokinins. *Methods in Molecular Biology,* **1569,** 31-39.

Dobrev PI, Kaminek M. 2002. Fast and efficient separation of cytokinins from auxin and abscisic acid and their purification using mixed-mode solid-phase extraction. *Journal of Chromatography A,* **950,** 21-9.

Dobrev PI, Vankova R. 2012. Quantification of abscisic Acid, cytokinin, and auxin content in salt-stressed plant tissues. *Methods in Molecular Biology*, **913,** 251-61.

Dong X, Hong Z, Chatterjee J, Kim S, Verma DP. 2008. Expression of callose synthase genes and its connection with Npr1 signaling pathway during pathogen infection. *Planta,* **229,** 87-98.

Ellinger D, Glockner A, Koch J, *et al.* 2014. Interaction of the Arabidopsis GTPase RabA4c with its effector PMR4 results in complete penetration resistance to powdery mildew. *Plant Cell,* **26,** 3185-200.

Ellinger D, Voigt CA. 2014. Callose biosynthesis in Arabidopsis with a focus on pathogen response: what we have learned within the last decade. *Annals of Botany,* **114,** 1349-58.

Ferrari S, Plotnikova JM, De Lorenzo G, Ausubel FM. 2003. Arabidopsis local resistance to Botrytis cinerea involves salicylic acid and camalexin and requires EDS4 and PAD2, but not SID2, EDS5 or PAD4. *Plant Journal,* **35,** 193-205.

Fujimoto M, Suda Y, Vernhettes S, Nakano A, Ueda T. 2015. Phosphatidylinositol 3-kinase and 4-kinase have distinct roles in intracellular trafficking of cellulose synthase complexes in Arabidopsis thaliana. *Plant and Cell Physiology,* **56,** 287-98.

Glazebrook J. 2005. Contrasting mechanisms of defense against biotrophic and necrotrophic pathogens. *Annual Review of Phytopathology,* **43,** 205-27.

Gross J, Cho WK, Lezhneva L, *et al.* 2006. A plant locus essential for phylloquinone (vitamin K1) biosynthesis originated from a fusion of four eubacterial genes. *Journal of Biological Chemistry,* **281,** 17189-96.

Chen XY, Kim JY. 2009. Callose synthesis in higher plants. *Plant Signaling and Behaviour,* **4,** 489-92.

Jacobs AK, Lipka V, Burton RA, *et al.* 2003. An Arabidopsis callose synthase, GSL5, is required for wound and papillary callose formation. *Plant Physiology*, **15**, 2503-2313.

Janda M, Sasek V, Ruelland E. 2014. The Arabidopsis pi4kIIIbeta1beta2 double mutant is salicylic acid-overaccumulating: a new example of salicylic acid influence on plant stature. *Plant Signaling and Behaviour*, **9,** e977210.

559 **Janda M, Ruelland E.** 2015. Magical mystery tour: salicylic acid signalling. *Environmental*
560 *and Experimental Botany*, **114,** 117-128.
561 **Kalachova T, Puga-Freitas R, Kravets V, *et al.*** 2016. The inhibition of basal
562 phosphoinositide-dependent phospholipase C activity in Arabidopsis suspension cells
563 by abscisic or salicylic acid acts as a signalling hub accounting for an important
564 overlap in transcriptome remodelling induced by these hormones. *Environmental and*
565 *Experimental Botany*, **123,** 37-49.
566 **Kang BH, Nielsen E, Preuss ML, Mastronarde D, Staehelin LA.** 2011. Electron
567 tomography of RabA4b- and PI-4Kbeta1-labeled trans Golgi network compartments in
568 Arabidopsis. *Traffic*, **12,** 313-29.
569 **Katagiri F, Thilmony R, He SY.** 2002. The Arabidopsis thaliana-pseudomonas syringae
570 interaction. *Arabidopsis Book*, **1,** e0039.
571 **Kohler A, Schwindling S, Conrath U.** 2002. Benzothiadiazole-induced priming for
572 potentiated responses to pathogen infection, wounding, and infiltration of water into
573 leaves requires the NPR1/NIM1 gene in Arabidopsis. *Plant Physiology*, **128,** 1046-56.
574 **Krinke O, Ruelland E, Valentová O, *et al.*** 2007. Phosphatidylinositol 4-Kinase activation is
575 an early response to salicylic acid in Arabidopsis suspension cells. *Plant Physiology*,
576 **144,** 1347-1359.
577 **Krinke O, Flemr M, Vergnolle C, *et al.*** 2009. Phospholipase D activation is an early
578 component of the salicylic acid signaling pathway in Arabidopsis cell suspensions.
579 *Plant Physiology*, **150,** 424-36.
580 **Lee H-A, Lee H-Y, Seo E, *et al.*** 2017. Current understandings of plant Nonhost Resistance.
581 *Molecular Plant-Microbe interactions*, **30**, 5-15

582 **Lin F, Krishnamoorthy P, Schubert V, *et al.*** 2019. A dual role for cell plate-associated
583 PI4Kβ in endocytosis and phragmoplast dynamics during plant somatic cytokinesis.
584 The EMBO journal, e100303.
585 **Luna E, Pastor V, Robert J, Flors V, Mauch-Mani B, Ton J.** 2011. Callose deposition: a
586 multifaceted plant defense response. *Molecular Plant-Microbe Interactions,* **24,** 183-
587 93.
588 **Mega R, Meguro-Maoka A, Endo A, *et al.*** 2015. Sustained low abscisic acid levels increase
589 seedling vigor under cold stress in rice (Oryza sativa L.). *Scientific Reports,* **5,** 13819.
590 **Mosher S, Moeder W, Nishimura N, *et al.*** 2010. The lesion-mimic mutant cpr22 shows
591 alterations in abscisic acid signaling and abscisic acid insensitivity in a salicylic acid-
592 dependent manner. *Plant Physiology,* **152,** 1901-13.
593 **Nakanishi S, Catt KJ, Balla T**. 1995. A wortmannin-sensitive phosphatidylinositol 4-kinase
594 that regulates hormone-sensitive pools of inositolphospholipids. *Proceedings of the*
595 *National Academy of Sciences of the USA,* **92**, 5317–5321.
596 **Noack LC, Jaillais Y.** 2017. Precision targeting by phosphoinositides: how PIs direct
597 endomembrane trafficking in plants. *Current Opinion in Plant Biology,* **40,** 22-33.
598 **Normanly J.** 2010. Approaching cellular and molecular resolution of auxin biosynthesis and
599 metabolism. *Cold Spring Harbor Perspectives in Biology,* **2,** a001594.
600 **Novakova M, Sasek V, Dobrev PI, Valentova O, Burketova L.** 2014. Plant hormones in
601 defense response of Brassica napus to Sclerotinia sclerotiorum - reassessing the role of
602 salicylic acid in the interaction with a necrotroph. *Plant Physiol Biochem,* **80,** 308-17.
603 **Pappan K, Austin-Brown S, Chapman KD, Wang X.** 1998. Substrate selectivities and lipid
604 modulation of plant phospholipase D alpha, -beta, and -gamma. *Archives of*
605 *Biochemistry and Biophysics,* **353,** 131-40.

606 **Platre MP, Jaillais Y.** 2016. Guidelines for the Use of Protein Domains in Acidic
607 Phospholipid Imaging. *Methods in Molecular Biology*, **1376,** 175-94.
608 **Preuss ML, Schmitz AJ, Thole JM, Bonner HK, Otegui MS, Nielsen E.** 2006. A role for
609 the RabA4b effector protein PI-4Kbeta1 in polarized expansion of root hair cells in
610 Arabidopsis thaliana. *Journal of Cell Biology*, **172,** 991-8.
611 **Sasek V, Janda M, Delage E, *et al.*** 2014. Constitutive salicylic acid accumulation in
612 pi4kIIIbeta1beta2 Arabidopsis plants stunts rosette but not root growth. *New*
613 *Phytologist*, **203,** 805-16.
614 **Seyfferth C, Tsuda K.** 2014. Salicylic acid signal transduction: the initiation of biosynthesis,
615 perception and transcriptional reprogramming. *Frontiers in Plant Science,* **5,** 697.
616 **Takemoto, D., Jones, D. A., & Hardham, A. R.** (2006). Re-organization of the cytoskeleton
617 and endoplasmic reticulum in the Arabidopsis pen1-1 mutant inoculated with the non-
618 adapted powdery mildew pathogen, *Blumeria graminis f. sp. hordei*. Molecular plant
619 pathology, 7(6), 553-563.
620 **Team RC.** 2014. R: A language and environment for statistical computing. R Foundation for
621 Statistical Computing. *Vienna, Austria*.
622 T**hiele K, Wanner G, Kindzierski V, *et al.*** 2009. The timely deposition of callose is
623 essential for cytokinesis in Arabidopsis. The Plant Journal, 58(1), 13-26.
624 **Tsuda K, Mine A, Bethke G, *et al.*** 2013. Dual regulation of gene expression mediated by
625 extended MAPK activation and salicylic acid contributes to robust innate immunity in
626 Arabidopsis thaliana. *PLoS Genetics*, **9,** e1004015.
627 **Vlot AC, Dempsey DA, Klessig DF.** 2009. Salicylic Acid, a Multifaceted Hormone to
628 Combat Disease. *Annual Review of Phytopathology*, **47,** 177-206.
629 **Vogel J, Somerville S.** 2000. Isolation and characterization of powdery mildew-resistant
630 Arabidopsis mutants. *Proceedings of the National Acadademy of Sciences U S A*, **97,**
631 1897-902.

Voigt CA. 2014. Callose-mediated resistance to pathogenic intruders in plant defense-related papillae. *Frontiers in Plant Science,* **5,** 168.

Wagner S, Stuttmann J, Rietz S, *et al.* 2013. Structural Basis for Signaling by Exclusive EDS1 Heteromeric Complexes with SAG101 or PAD4 in Plant Innate Immunity. *Cell Host & Microbe,* **14,** 619-630.

Wildermuth MC, Dewdney J, Wu G, Ausubel FM. 2001. Isochorismate synthase is required to synthesize salicylic acid for plant defence. *Nature,* **414,** 562-5.

Yi SY, Shirasu K, Moon JS, Lee SG, Kwon SY. 2014. The activated SA and JA signaling pathways have an influence on flg22-triggered oxidative burst and callose deposition. *PLoS One,* **9,** e88951.

Zhang Z, Feechan A, Pedersen C, *et al.* 2007. A SNARE-protein has opposing functions in penetration resistance and defence signalling pathways. *Plant Journal,* **49,** 302-12.

FIGURE CAPTIONS

Figure 1. Correlation matrix between phytohormones levels. The matrix was built using the Pearson correlation of 27 hormone-related metabolites from 24 independent samples corresponding to 6 genotypes (WT; *sid2*; *NahG*; *pi4kβ1β2*; *sid2pi4kβ1β2; NahGpi4kβ1β2*; four plants per genotype). Positive correlations are displayed in blue and negative correlations in red. Colour intensity and the size of the circles are proportional to the correlation coefficients. Red rectangles highlight the correlation between SA and other hormones.

Figure 2. Resistance to biotic stresses of *pi4kβ1β2* and s*id2pi4kβ1β2 m*utants. A. Resistance to biotroph *H. arabidopsidis*. B. Resistance to hemibiotroph *Pseudomonas syringae* pv. *syringae* DC3000. Infiltration treatment of 4 week-old-plants, with 6 independent samples. C.

Resistance to the necrotroph *Botrytis cinerea*. 4-5-week-old *A. thaliana* were inoculated with a 6 µL drop containing spores of *B. cinerea* (50000 spores per mL), placed into a plastic box and kept in the dark for 56 h. Statistical differences between the genotypes for B and C were assessed using ANOVA, with a Tukey honestly significant difference (HSD) multiple mean comparison *post hoc* test. Different letters indicate a significant difference, Tukey HSD, $P < 0.05$, n=10 for A, n=7 for B and n=27 for C.

Figure 3. Pattern of callose accumulation in *pi4kβ1β2* leaves. A. Aniline blue staining, and fluorescent microscopy. The bar corresponds to 500 µm. B. Callose particles accumulated in different ROI. The squares represent the ROI. Data are presented as means ±SEM. Statistical differences were assessed using a two-way ANOVA, with a Tukey honestly significant difference (HSD) multiple mean comparison *post hoc* test. Different letters indicate a significant difference, Tukey HSD, $P < 0.05$. n=11.

Figure 4. Callose deposition in response to flagellin. A. Representative images of callose accumulated in leaves of 4-week-old *A. thaliana* plants by aniline blue staining, 24 h after infiltration with 0.1 µM flg22 or mock infiltration. The bar = 1cm. B. Quantification of callose particles. Values represent an average of 5 ROI. Data are presented as means +SD. For each treatment, statistical differences between the genotypes were assessed using a one-way ANOVA, with a Tukey honestly significant difference (HSD) multiple mean comparison *post hoc* test. Different letters indicate a significant difference, Tukey HSD, $P < 0.01$, n=4.

Figure 5. Resistance of *pi4kβ1β2* to penetration by the non-host pathogen *Blumeria graminis* f. sp. *Hordei* (*Bgh*). A. Four types of interactions counted in the penetration success analysis

after trypan blue staining. Scale bar represents 5 µm. B. Data showing penetration success of *Bgh* 24 hpi in each genotype, the mean number of cells with either haustoria or dead cells, respectively. C. Data show mean area of a callose spot per mm^2 at 24hpi after interaction with *Bgh* spores. D. Data show mean area of a callose spot per mm^2 at 24hpi after interaction with *Bgh* spores. Data at B, C and D were processed by ANOVA, with a Tukey honestly significant difference (HSD) multiple mean comparison *post hoc* test, the data represent 1 independent experiment, the experiment was repeated four times. The letters indicate significant difference Tukey HSD, $P < 0.01$. E. Pictures demonstrating callose staining with aniline blue 24 hpi with *Bgh*. Scale bar 100 µm.

Figure 6. Schematic representation of the effects of the *pi4kβ1β2* double mutation on Arabidopsis plants.

SUPPLEMENTARY DATA

Supplemental Table S1. Phytohormone levels in 4-week-old plants. Values are expressed in pmol/gFW. For each genotype, 4 plants were assessed.

Fig. S1: Levels of hormones controlled by SA in four-week-old mutant and WT plants. Values represent means and SEM from four samples. For each hormone, statistical differences between the genotypes were assessed using a one-way ANOVA, with a Tukey honestly significant difference (HSD) multiple mean comparison *post hoc* test. Different letters indicate a significant difference, Tukey HSD, $P < 0.05$. n=4. Note the broken y-axis due to high SA in the *npr1pi4kβ1β2* triple mutant.

Fig. S2. Levels of hormones not controlled by SA in four-week-old mutant and WT plants. For each hormone, statistical differences between the genotypes were assessed using a one-

706 way ANOVA, with a Tukey honestly significant difference (HSD) multiple mean comparison
707 *post hoc* test. Different letters indicate a significant difference, Tukey HSD, $P < 0.05$. n=4.
708 Fig. S3. Resistance to *P. syringae* pv. *tomato* DC3000 AvrRpt2. 4-week-old *A. thaliana*
709 plants were infiltrated with a bacterial suspension. Data show infection development at 2 dpi.
710 Fig. S4. Callose deposition in response to wounding. A. Representative images of callose
711 accumulated in leaves of 4-week-old *A. thaliana* plants 24 h after infiltration with a needless
712 syringe, leaf area outside of the place of infiltration ('mock") or at the very place of treatment
713 ("wounding"). Aniline blue staining, bar=1cm. B. Quantification of callose particles. Data are
714 given as means +SD. For each treatment, statistical differences between the genotypes were
715 assessed using a one-way ANOVA, with a Tukey honestly significant difference (HSD)
716 multiple mean comparison *post hoc* test. Different letters indicate a significant difference,
717 Tukey HSD, $P < 0.01$, n=4.
718 Fig. S5. Relative transcription of some *CalS* genes in untreated rosette leaves or 24h after
719 infiltration with 0.1µM flg22.

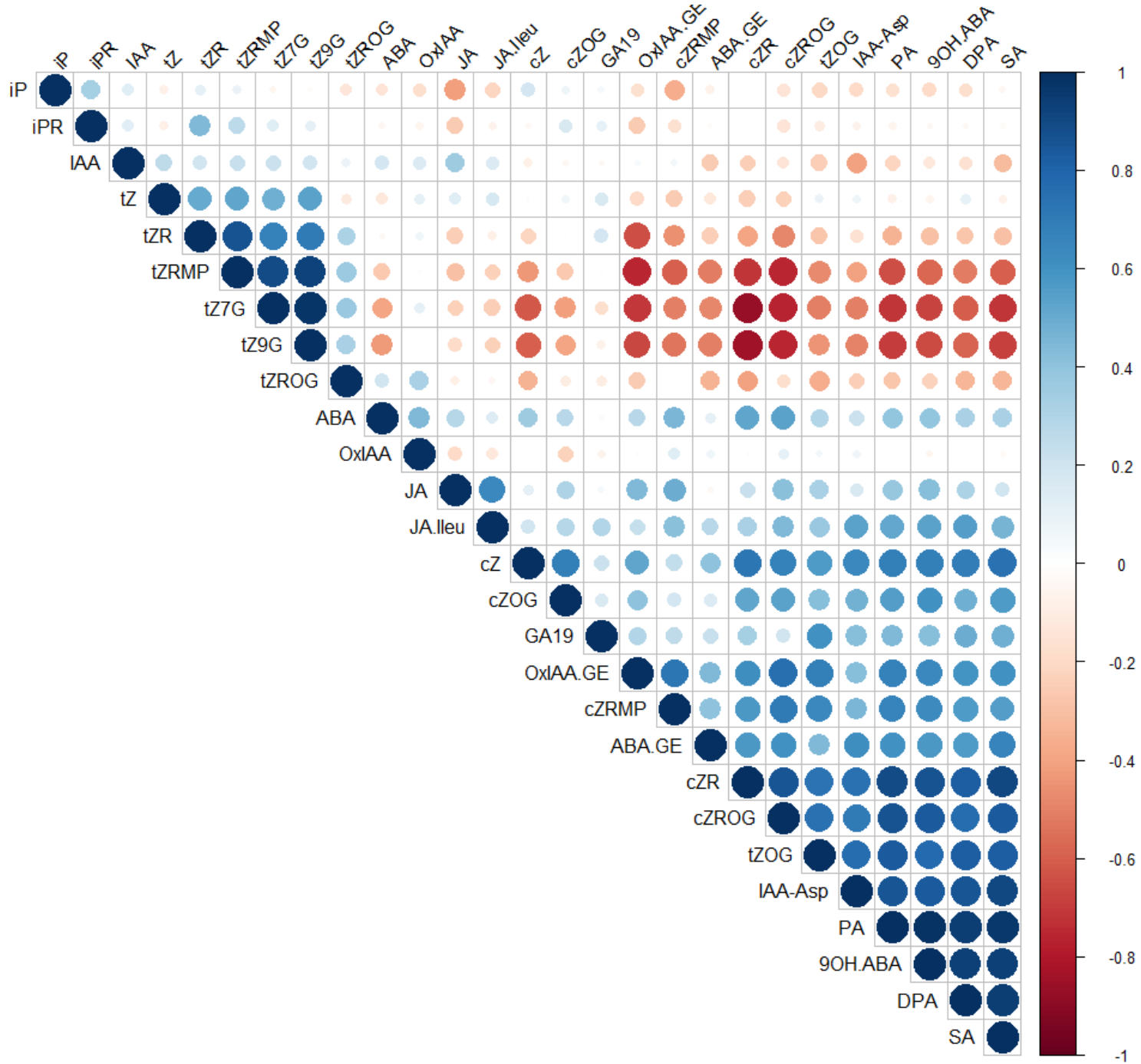
iP
iPR
IAA
tZ
tZR
tZRMP
tZ7G
tZ9G
tZROG
ABA
OxIAA
JA
JA.Ileu
cZ
cZOG
GA19
OxIAA.GE
cZRMP
ABA.GE
cZR
cZROG
tZOG
IAA-Asp
PA
9OH.ABA
DPA
SA
1
0.8
0.6
0.4
0.2
0
-0.2
-0.4
-0.6
-0.8
-1

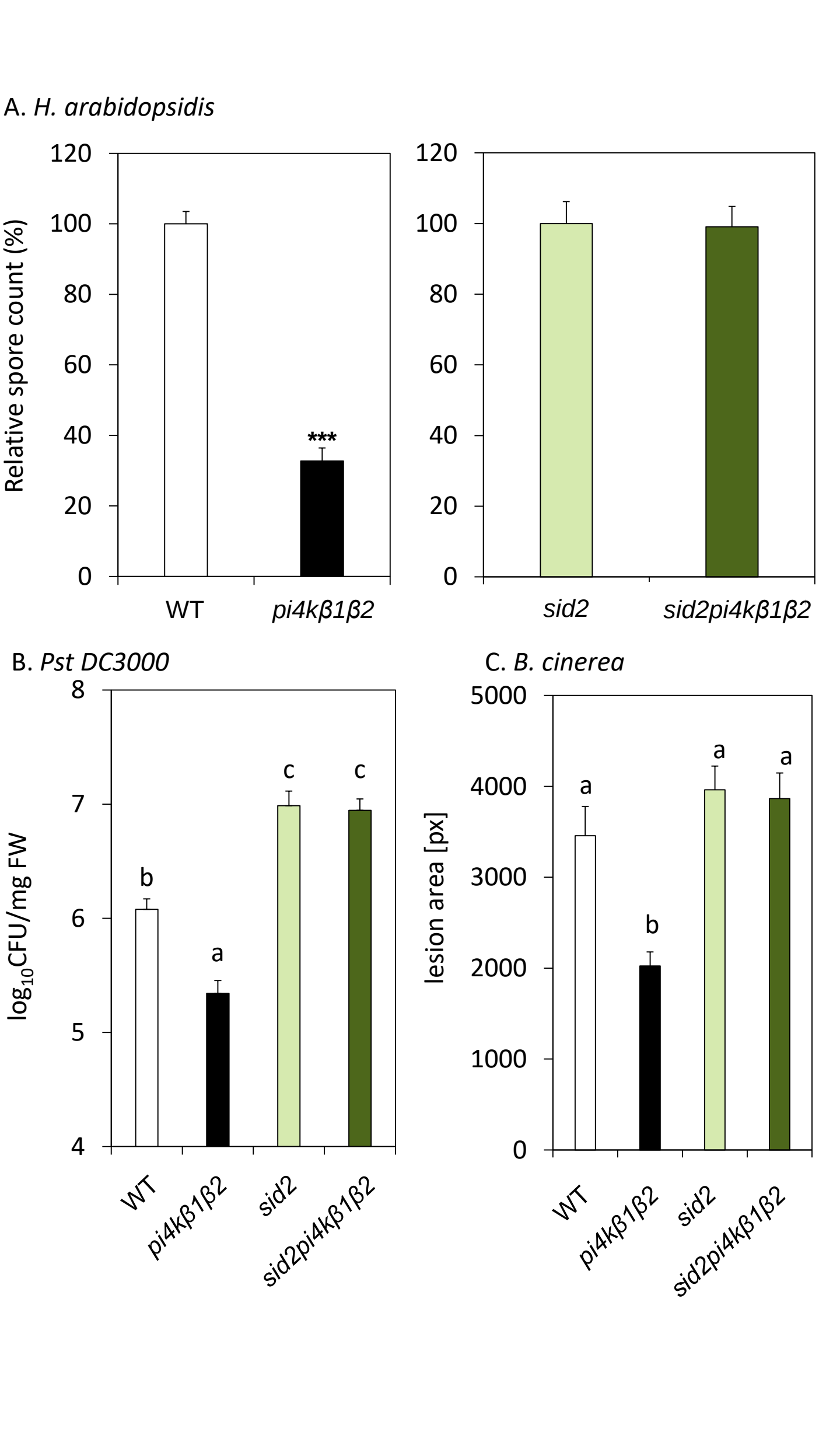
A. H. arabidopsidis
Relative spore count (%)
120
100
80
60
40
20
0
***
WT
pi4kβ1β2
sid2
sid2pi4kβ1β2
B. Pst DC3000
log10CFU/mg FW
8
7
6
5
4
b
a
c
c
WT
pi4kβ1β2
sid2
sid2pi4kβ1β2
C. B. cinerea
lesion area [px]
5000
4000
3000
2000
1000
0
a
b
a
a
WT
pi4kβ1β2
sid2
sid2pi4kβ1β2

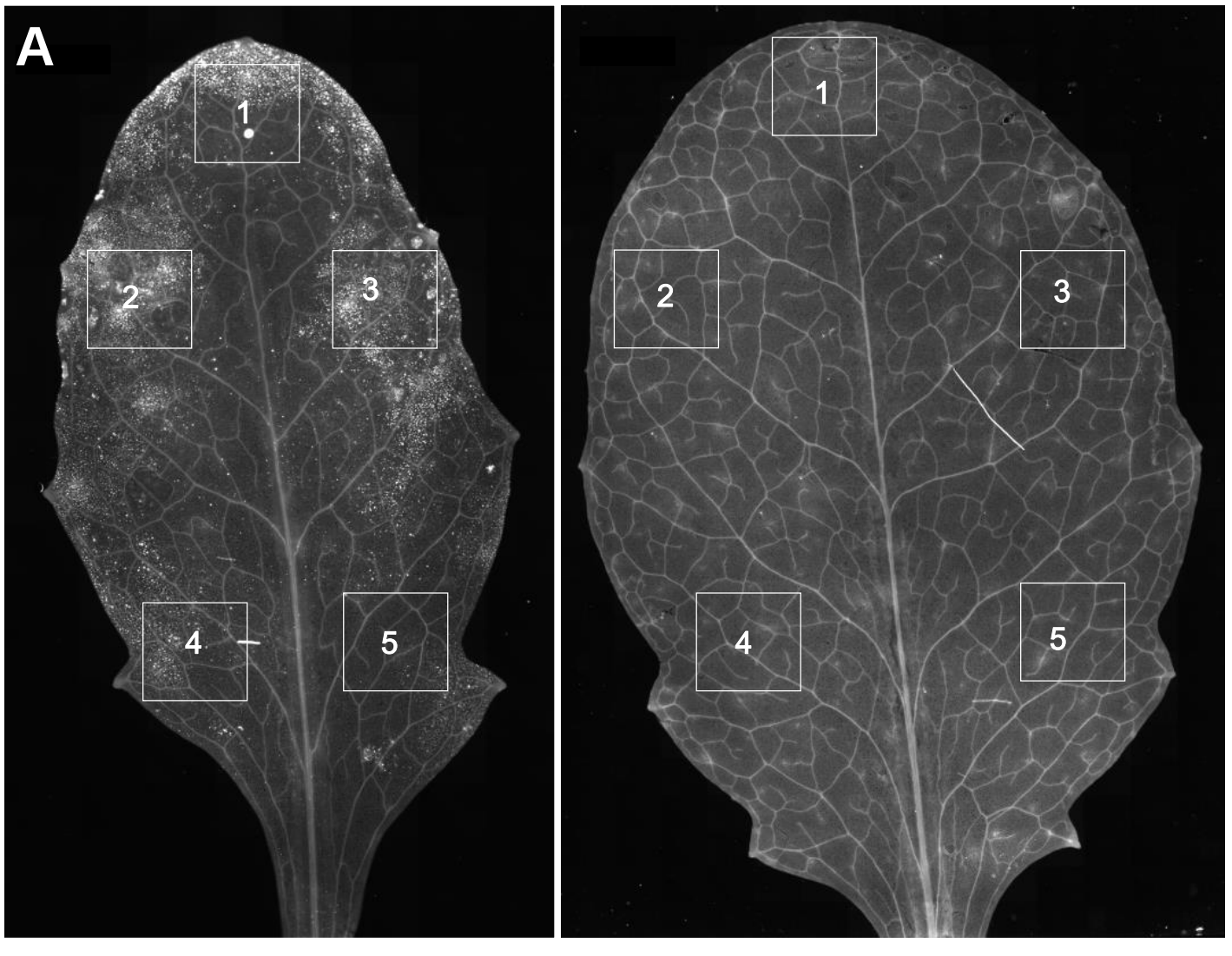
A
1
2
3
4
5
1
2
3
4
5
pi4kβ1β2
WT

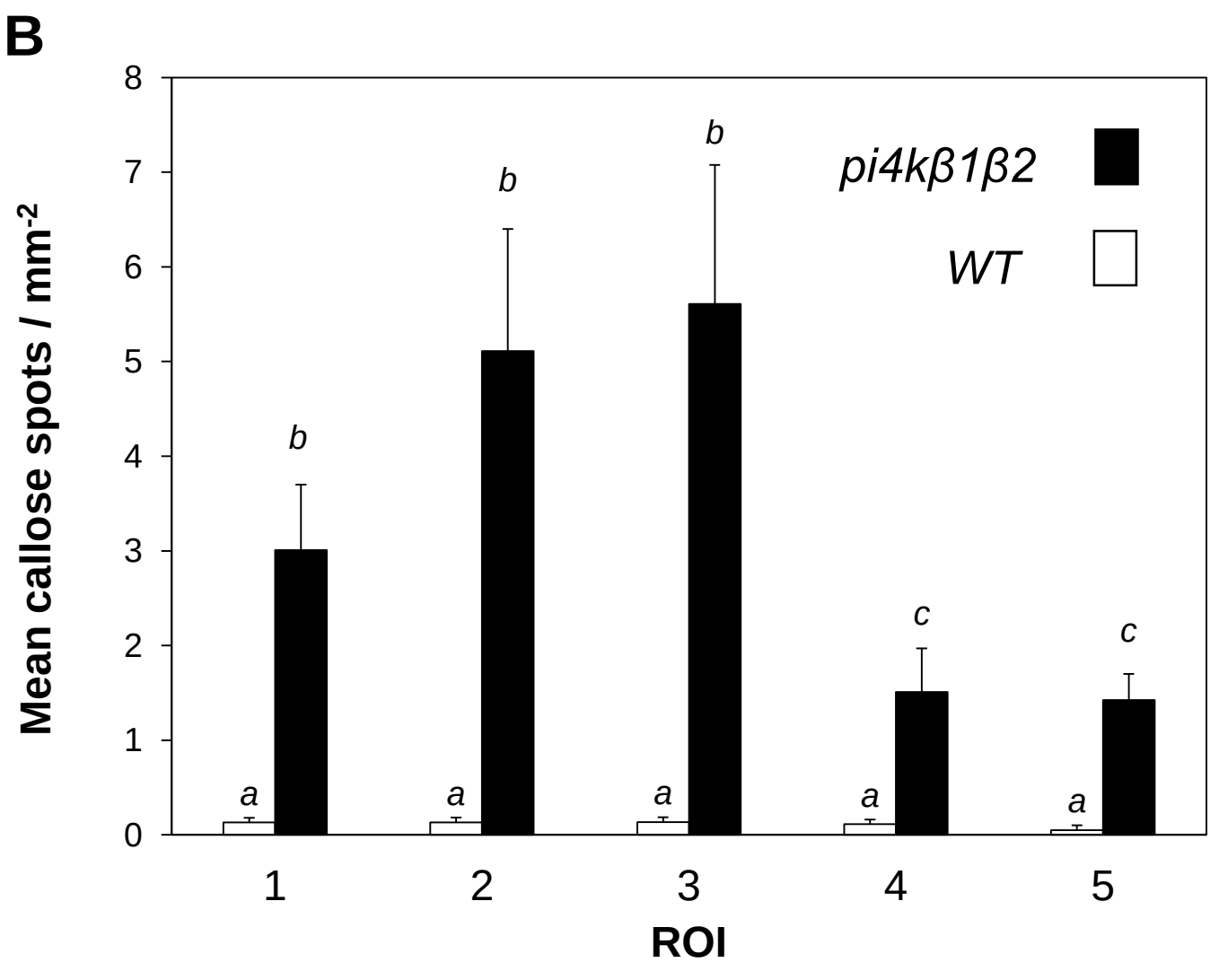
B
Mean callose spots / mm-2
0
1
2
3
4
5
6
7
8
a
b
a
b
a
b
a
c
a
c
pi4kβ1β2
WT
1
2
3
4
5
ROI

A.

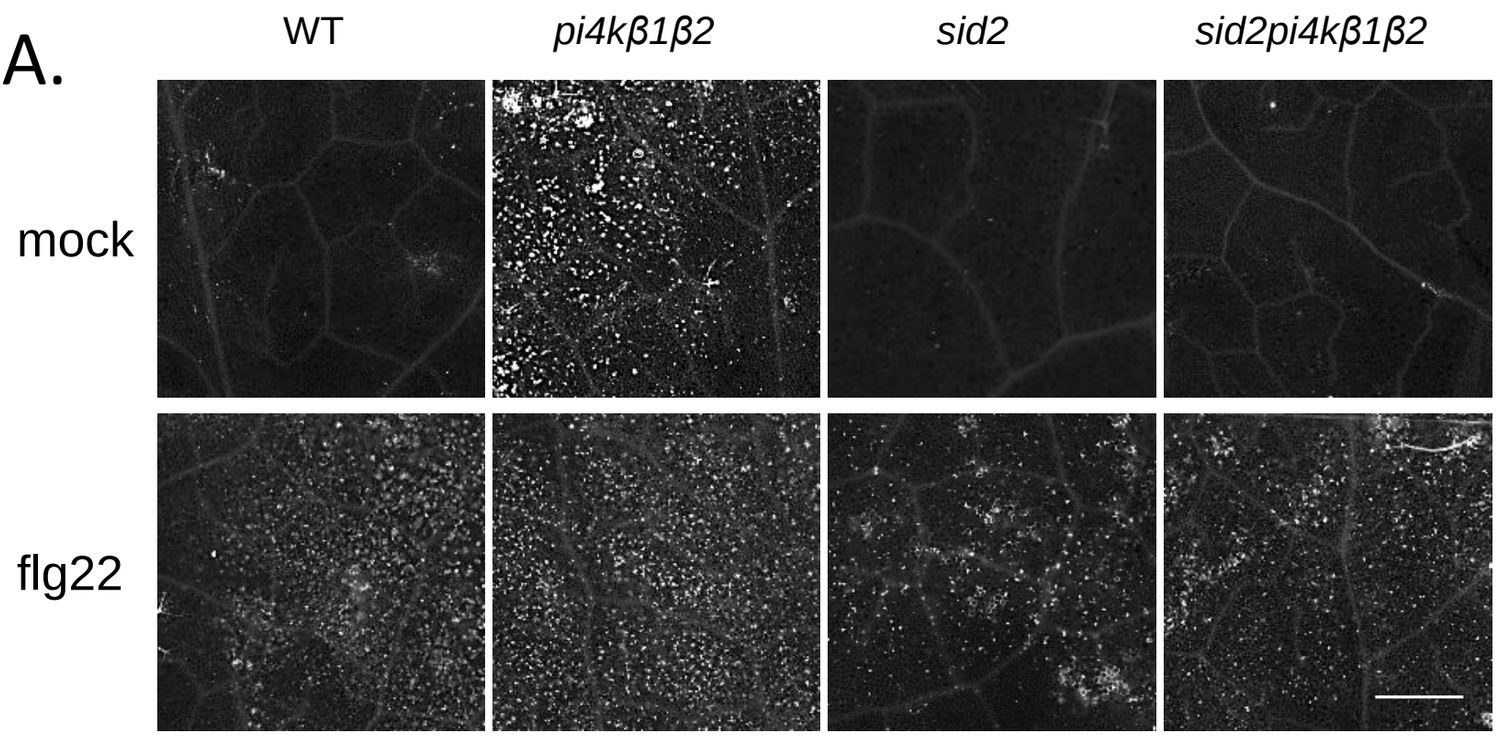
WT
pi4kβ1β2
sid2
sid2pi4kβ1β2
mock
flg22

B.

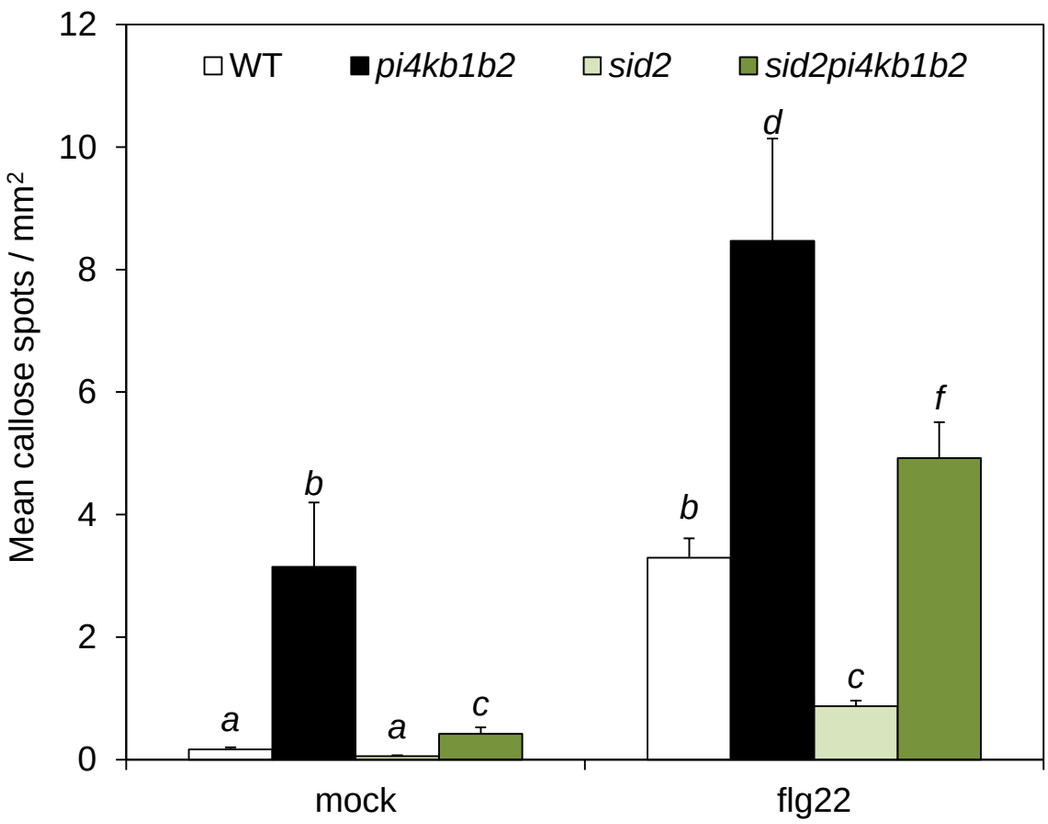
WT
pi4kb1b2
sid2
sid2pi4kb1b2
Mean callose spots / mm²
0
2
4
6
8
10
12
a
b
a
c
b
d
c
f
mock
flg22

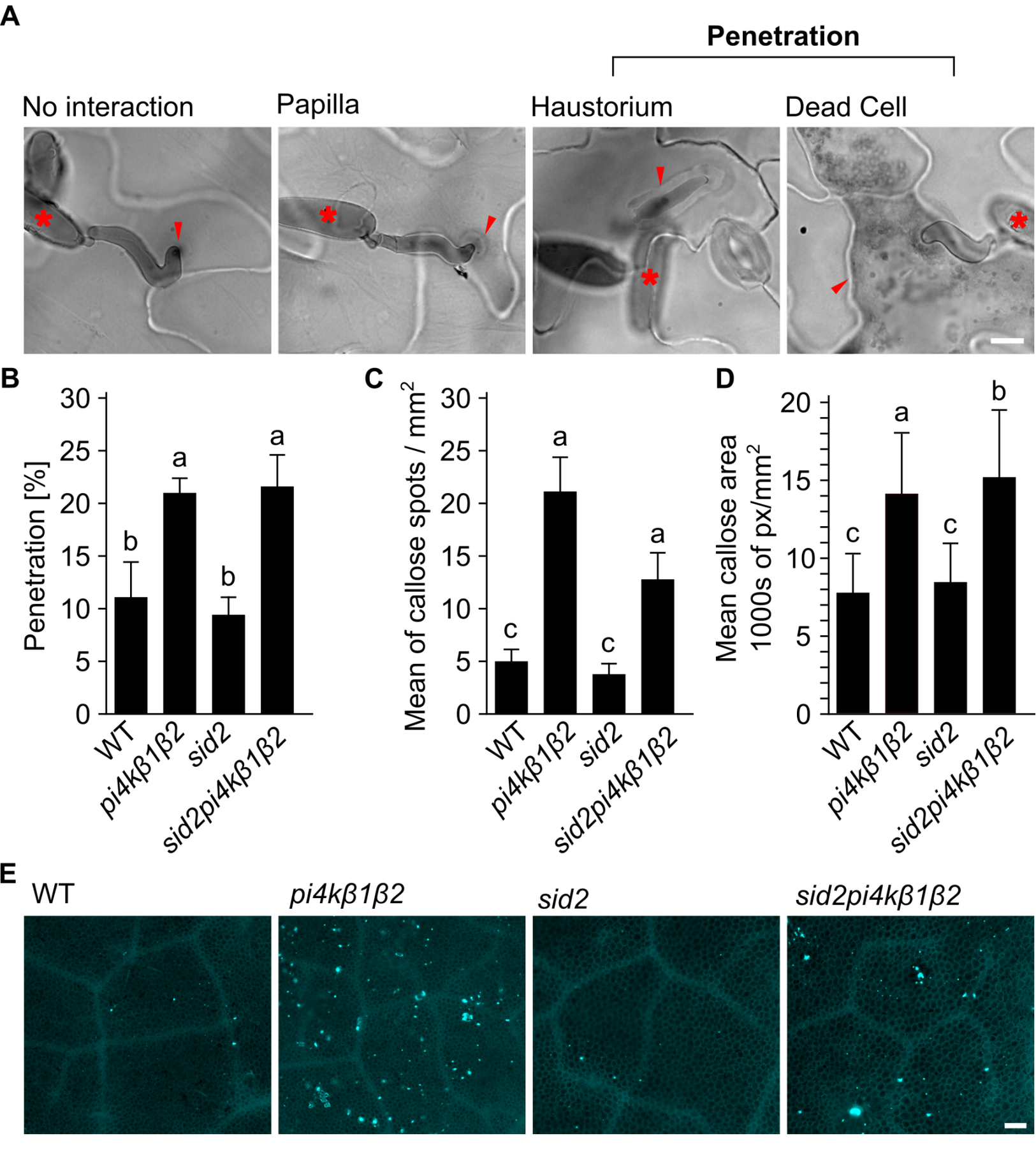
A
Penetration
No interaction
Papilla
Haustorium
Dead Cell
B
Penetration [%]
C
Mean of callose spots / mm2
D
Mean callose area
1000s of px/mm2
WT
pi4kβ1β2
sid2
sid2pi4kβ1β2
E
WT
pi4kβ1β2
sid2
sid2pi4kβ1β2

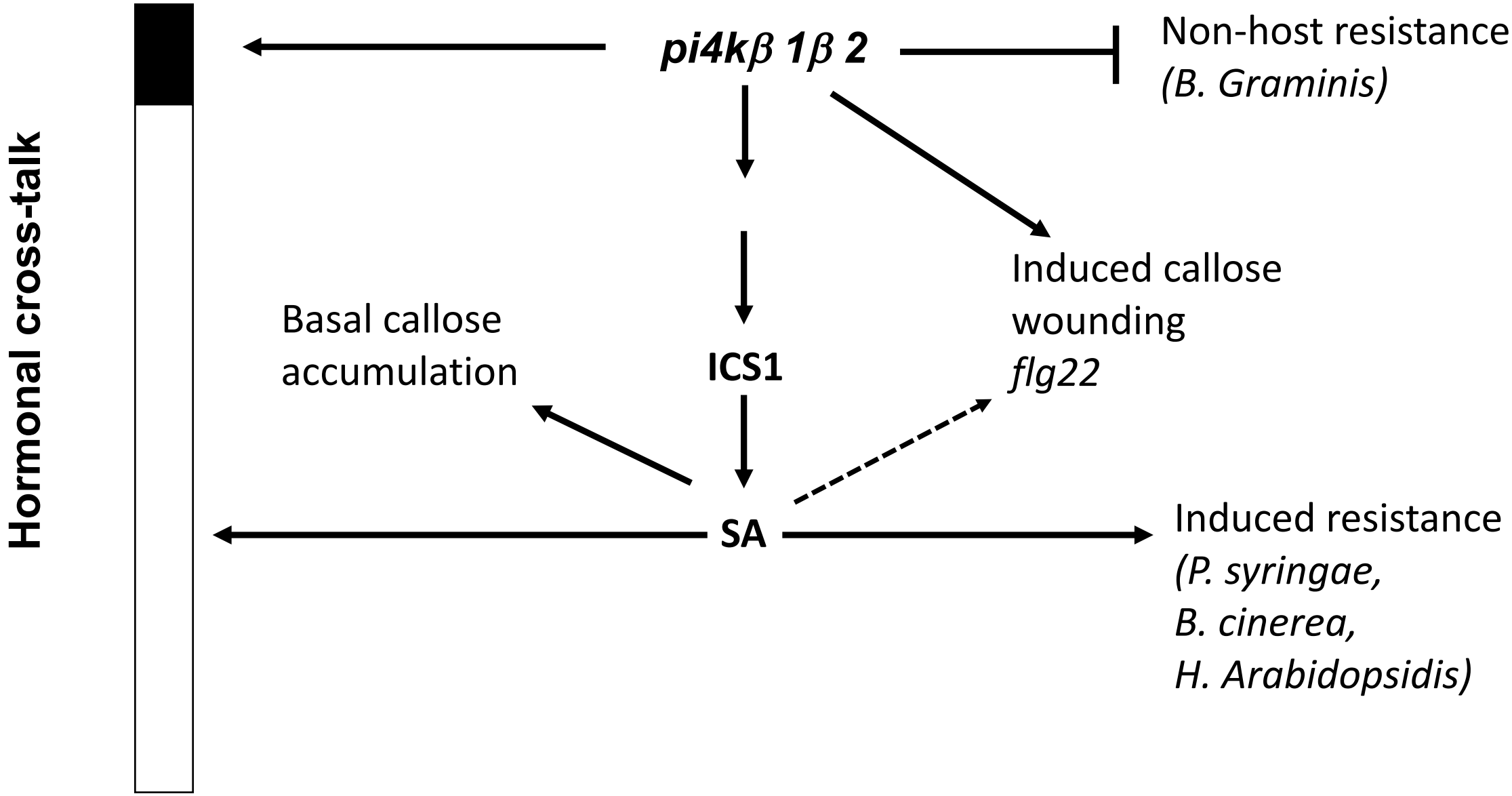
Hormonal cross-talk
pi4kβ 1β 2
Non-host resistance
(B. Graminis)
Induced callose
wounding
flg22
Basal callose
accumulation
ICS1
SA
Induced resistance
(P. syringae,
B. cinerea,
H. Arabidopsidis)